Published in final edited form as:
JACC Cardiovasc Imaging. 2011 March ; 4(3): 269–278. doi:10.1016/j.jcmg.2010.09.023.

Direct T2 Quantification of Myocardial Edema in Acute Ischemic Injury

David Verhaert, MD, **Paaladinesh Thavendiranathan, MD**, **Shivraman Giri, MS**, **Georgeta Mihai, PhD**, **Sanjay Rajagopalan, MD**, **Orlando P. Simonetti, PhD**, and **Subha V. Raman, MD, MSEE**
The Ohio State University, Columbus, Ohio

Abstract

OBJECTIVES—To evaluate the utility of rapid, quantitative T2 mapping compared with conventional T2-weighted imaging in patients presenting with various forms of acute myocardial infarction.

BACKGROUND—T2-weighted cardiac magnetic resonance (CMR) identifies myocardial edema before the onset of irreversible ischemic injury and has shown value in risk-stratifying patients with chest pain. Clinical acceptance of T2-weighted CMR has, however, been limited by well-known technical problems associated with existing techniques. T2 quantification has recently been shown to overcome these problems; we hypothesized that T2 measurement in infarcted myocardium versus remote regions versus zones of microvascular obstruction in acute myocardial infarction patients could help reduce uncertainty in interpretation of T2-weighted images.

METHODS—T2 values using a novel mapping technique were prospectively recorded in 16 myocardial segments in 27 patients admitted with acute myocardial infarction. Regional T2 values were averaged in the infarct zone and remote myocardium, both defined by a reviewer blinded to the results of T2 mapping. Myocardial T2 was also measured in a group of 21 healthy volunteers.

RESULTS—T2 of the infarct zone was 69 ± 6 ms compared with 56 ± 3.4 ms for remote myocardium ($p < 0.0001$). No difference in T2 was observed between remote myocardium and myocardium of healthy volunteers (56 ± 3.4 ms and 55.5 ± 2.3 ms, respectively, p = NS). T2 mapping allowed for the detection of edematous myocardium in 26 of 27 patients; by comparison, segmented breath-hold T2-weighted short tau inversion recovery images were negative in 7 and uninterpretable in another 2 due to breathing artifacts. Within the infarct zone, areas of microvascular obstruction were characterized by a lower T2 value (59 ± 6 ms) compared with areas with no microvascular obstruction (71.6 ± 10 ms, $p < 0.0001$). T2 mapping provided consistent high-quality results in patients unable to breath-hold and in those with irregular heart rhythms, in whom short tau inversion recovery often yielded inadequate imaging.

Reprint requests and correspondence: Dr. Subha V. Raman, Davis Heart and Lung Research Institute, The Ohio State University, 473 West 12th Avenue, Suite 200, Columbus, Ohio 43210. raman.1@osu.edu.

The other authors have reported that they have no relationships to disclose.

CONCLUSIONS—Quantitative T2 mapping reliably identifies myocardial edema without the limitations encountered by T2-weighted short tau inversion recovery imaging, and may therefore be clinically more robust in showing acute ischemic injury.

Keywords

acute myocardial infarction; cardiac magnetic; resonance; edema; T2

The identification of reversible injury by T2-weighted cardiac magnetic resonance imaging (CMR) leverages the well-established phenomenon of increased myocardial free water in the setting of acute ischemia (1), taking advantage of the established relationship between T2 signal intensity and tissue water content (2). Myocardial T2 is not only determined by an absolute increase in myocardial water, but also by the movement of water molecules from the extracellular to the intracellular environment (cellular edema) and by the dissociation of water molecules from proteins leading to free instead of bound water (3). Recent studies showed myocardial T2 to increase not only with acute myocardial infarction (AMI), but also with severe transient ischemia (4–6). Furthermore, it has been reported that T2 signal hyperintensity may identify myocardial ischemia even before detectable injury by troponin or late gadolinium enhancement (LGE) (4). These observations have important clinical implications because patients with myocardium at risk are generally expected to benefit from early diagnosis and prompt intervention to arrest the process of cell death. However, several problems inherent to T2-weighted CMR have limited the widespread clinical acceptance of this sequence to detect edema in patients with acute coronary syndromes; these include surface coil intensity variation, bright signal from stagnant blood potentially interfering with elevated T2 in the subendocardium, motion artifacts, and the subjective nature of T2-weighted CMR image interpretation (7,8). Our group recently developed a novel quantitative T2-mapping technique that overcomes these limitations (9). In this work, we applied this technique to test the diagnostic utility of T2 mapping compared with T2-weighted CMR in patients with recent AMI.

METHODS

Study population

Patients with AMI as defined by established diagnostic criteria (10) were prospectively enrolled. Both ST-segment elevation myocardial infarction (STEMI) and non–ST-segment elevation myocardial infarction (NSTEMI) patients were considered eligible. In addition, healthy volunteers with no cardiovascular history were recruited to undergo myocardial T2 mapping alone in a single mid-ventricular short axis plane.

In patients, medical history, clinical and electrocardiographic findings, as well as serological markers were recorded at entry. Contraindications to CMR such as pacemaker and hemodynamic instability constituted exclusion criteria. All patients provided written informed consent to participate in this institutional review board–approved protocol.

CMR examination

Examinations were performed using a 1.5-T CMR system and 12-element phased-array cardiac coil (MAGNETOM Avanto, Siemens Medical Solutions, Inc., Erlangen, Germany). A physician provided monitoring throughout the study. The following CMR protocol was used:

1. Multiplane, balanced steady-state free precession (SSFP) cine imaging suitable for wall motion assessment and volumetric analysis. Cine images were obtained in the horizontal long-axis, vertical long-axis, 3-chamber, and contiguous short-axis planes. Real-time cine imaging with a TSENSE acceleration factor of 3 was used for subjects unable to breath-hold.
2. T2-weighted short tau inversion recovery (T2-STIR) images obtained in basal, mid, and apical short-axis, vertical long-axis, 3-chamber, and horizontal long-axis planes (11).
3. T2 maps acquired in the same planes as the T2-STIR images using a T2-prepared single-shot SSFP sequence as previously described in detail (9). Briefly, T2 maps were generated by acquiring three T2-weighted images, each image with a different T2 preparation time (0 ms, 24 ms, and 55 ms, respectively; repetition time = 3 × R-R, total acquisition time of 7 heart-beats). To correct for motion between images, a fast variational nonrigid registration algorithm was used, aligning all T2-prepared frames to the center frame (12). The signal intensity of corresponding pixels in the 3 images, thus becoming a function of T2 decay, was then fitted using a linear 2-parameter model after logarithmic transformation to derive the T2 value of each pixel.
4. Multiplane LGE imaging using a segmented inversion-recovery gradient-echo sequence 10 min after 0.2 mmol/kg gadolinium– diethylene-triaminepentaacetic acid administration. Images were obtained in the same planes as SSFP cine images, with the inversion time adjusted to null normal myocardium. Non–breath-hold single-shot LGE imaging was performed for patients with limited breath-hold capacity (13).

Typical parameters for the sequences that were used are shown in Table 1.

Image analysis

Left ventricular (LV) end-diastolic volumes, end-systolic volumes, and mass were measured using Simpson’s method and indexed according to body surface area. The standard 17-segment model (14) was used to evaluate regional wall motion (0, normal; 1, mild or moderate hypokinesia; 2, severe hypokinesia; 3, akinesia; 4, dyskinesia), and the wall motion score index was calculated as the sum of segmental scores divided by 17. Regional function was also assessed by analyzing peak circumferential and radial strain in each segment from a basal, mid, and apical short-axis breath-hold SSFP cine slice using a vector-based feature tracking software (Vector Velocity Imaging, Siemens, Mountain View, California) that previously has been validated and described in detail (15). Briefly, a contour manually drawn along the LV endocardial border is automatically propagated by the

software, which divides the ventricle into 6 equiangular segments. By tracking the features within each voxel throughout the rest of the cardiac cycle (similar to speckle tracking in echocardiography), the software derives circumferential and radial strain values for each of the 16 LV segments (2 septal and 2 lateral segments in the apex were averaged to generate 4 apical segments).

The extent of hyperenhanced tissue on LGE imaging within each myocardial segment was rated visually using a 5-point scale (0, no hyperenhancement; 1, 1% to 25% hyperenhancement; 2, 26% to 50% hyperenhancement; 3, 51% to 75% hyperenhancement; and 4, 76% to 100% hyperenhancement); segmental LGE scores were subsequently summed to yield patient-level aggregate scores (16). Microvascular obstruction (MO) was defined as dark central areas surrounded by hyperenhanced necrotic myocardium on LGE imaging.

T2 values were similarly recorded from the quantitative T2 maps for each segment except for the true apex (segment 17), which was avoided due to partial volume effects that made it difficult to mark the myocardial border in this inherently thin myocardial region. Differences in quantitative T2 between corresponding segments in short-axis and long-axis views are usually small and nonsignificant at the basal and mid-ventricular level, but higher at the apex due to the effects of partial volume averaging, as we have shown previously (9). To limit the effects of partial volume averaging, T2 values in the apical segments were derived from long-axis views (horizontal and vertical long axes) solely.

For healthy volunteers, myocardial T2 was measured by drawing a region of interest encompassing all myocardium.

T2-STIR images were independently evaluated by 2 experienced reviewers (D.V., S.V.R.) and rated by consensus as positive for edema, negative for edema, or unassessable.

A third reviewer (P.T.), blinded to the results of T2 mapping and regional strain analysis, then defined on a 16-segment model areas representing the infarct zone and areas considered to represent remote myocardium. This was accomplished by reviewing the patients' cine images, LGE information, and pertinent clinical information including electrocardiograms and coronary angiograms.

Segmental T2 values as well as segmental values for peak circumferential and radial strain that previously had been obtained according to the 16-segment model were then averaged for the infarct zone and remote myocardium as defined by the blinded assessment.

Statistical analysis

Continuous data with normal distribution are expressed as mean ± SD and non-normally distributed data as median and inter-quartile range. Categorical data are expressed as frequency or percentage. The mean values of continuous variables with normal distribution were compared using a 2-sample *t* test or paired *t* test, as appropriate. Correlation between continuous variables was computed with the Spearman rank correlation coefficient. Categorical variables were compared using the Fisher exact test. Interobserver variability

was tested by Bland-Altman analysis. Statistical significance was set at a 2-tailed probability level of <0.05. The authors had full access to the data and take responsibility for its integrity.

RESULTS

Study population

The baseline characteristics of 27 patients who presented with AMI are summarized in Table 2. The majority of patients included in this study did not have a history of cardiac events before their current admission. CMR was performed in all patients after they underwent coronary angiography, but revascularization was not pursued in 7 (1 STEMI and 6 NSTEMI) patients. Additionally, T2 maps were acquired in 13 male and 8 female healthy volunteers age 28 ± 7 years. All patients and control subjects were in sinus rhythm at the time of CMR examination.

LV structure, function, and irreversible injury

The routine CMR findings in our study population are shown in Table 3. Non–breath-hold real-time SSFP cine imaging and single-shot LGE imaging were used in a total of 5 subjects experiencing shortness of breath.

Global LV systolic function was overall slightly decreased, with LV ejection fraction averaging 49%; 96% of patients had at least 1 dysfunctional LV segment. Two patients (1 STEMI patient who underwent successful revascularization within 60 min of symptom onset and 1 patient presenting with NSTEMI) did not have evidence of infarct scar by LGE. As expected, LGE score increased with increasing peak troponin level ($r2 = 0.45$, $p = 0.0002$). In the subgroup of patients undergoing breath-hold SSFP cine imaging ($n = 22$), the mean difference in peak circumferential and radial strain between infarct and remote myocardium was −10.9% (95% confidence interval [CI]: −7.9% to −13.9%, $p < 0.0001$) and 24.3% (95% CI: 18.3% to 30.4%, $p < 0.0001$), respectively, confirming that remote and infarcted myocardial regions were accurately identified.

T2 mapping

The results of quantitative T2 mapping are shown in Figure 1. The mean T2 measured within the infarct zone was 69 ± 6 ms compared with 56 ± 3.4 ms in remote myocardium ($p < 0.0001$). Typical examples of T2 maps compared with T2-STIR and LGE images are shown in Figure 2. Overall, for the entire study population, almost no overlap was observed between T2 values measured in the infarct region and remote myocardium. In 1 patient with cocaine-induced myocardial infarction complicated by sustained ventricular tachycardia requiring electrical cardioversion before CMR evaluation, relatively high T2 values were measured in the remote segments (64 ms). However, in this case, it was still possible to demarcate the infarct zone by T2 mapping (infarct T2: 87 ms). Interestingly, this patient and 1 other patient with markedly elevated T2 in the infarct zone (86 ms) exhibited increased signal intensity of the infarct zone by SSFP imaging, suggesting the presence of extensive tissue edema. SSFP imaging did not show increased signal in any other patients, consistent with the known insensitivity of this technique to less extensive tissue edema.

No significant difference was found in T2 between the myocardium of healthy subjects and remote myocardium of infarct patients (55.5 ± 2.3 ms vs. 56 ± 3.4 ms, respectively; p = NS) (Fig. 1).

MO and the effect on T2

Overall, 13 patients had evidence of MO on LGE imaging (10 with STEMI, 3 with NSTEMI). When comparing T2 maps with matching LGE images, T2 values in segments with extensive MO were lower compared with the T2 values measured in the infarct outside the MO area (Fig. 3). In this subset of patients with evidence of MO, the mean T2 was 58.7 ± 6 ms within the area of MO compared with 71.3 ± 10 ms for infarct tissue outside the area of MO ($p < 0.0001$; Fig. 4).

T2-STIR imaging versus T2 mapping

T2 maps could be obtained in all subjects, and in 26 of 27 patients (96%), it was possible to differentiate injured from remote myocardium on the basis of segmental T2 values alone. In contrast, initial attempts to acquire T2-STIR images were stopped in 2 patients who were unable to breath-hold because of severe respiratory motion artifacts leading to uninterpretable results. Of the remaining 25 patients, it was possible to detect myocardial edema as areas of T2-STIR signal hyperintensity in 18 patients (72%). Remarkably, in 1 of the 2 patients with SSFP signal hyperintensity and very high T2 in the infarct zone (the cocaine-related case), T2-STIR images were nondiagnostic.

Overall, in the entire population, edema was more frequently detected by T2-STIR in patients presenting with STEMI compared with NSTEMI patients (88% vs. 36%, p = 0.01). Importantly, in all 7 patients with negative T2-STIR images, clear differences could be observed in quantitative T2 between infarct and remote myocardium using the T2 mapping sequence (Fig. 5).

Interobserver variability

Interobserver variability analysis was performed in all patients and healthy controls by 2 independent observers. In patients, infarct zone and remote myocardium were defined on the basis of previous description. In healthy controls, myocardial T2 values were measured by drawing a region of interest encompassing all myocardium from a mid-ventricular short-axis slice. Respective Bland-Altman plots for remote myocardium, infarcted segments, and control patients are shown in Figure 6. The mean difference between the 2 readers was 0.2 ms in infarcted segments (95% CI: −0.9 ms to 0.5 ms), 0.3 ms in remote myocardium (95% CI: −0.8 ms to 0.4 ms), and 0.4 ms in control patients (95% CI: −0.3 ms to 1.1 ms).

DISCUSSION

The detection of myocardial edema using a dark blood turbo spin-echo technique has previously been shown to allow early diagnosis of acute coronary syndromes and may identify both the area at risk and the amount of myocardial salvage post-reperfusion (4,5,17). Nevertheless, the applicability and clinical acceptance of T2-STIR imaging for exactly these purposes have been challenged by a set of problems that are widely recognized

(7,8). These include the sensitivity of the sequence to artifacts from respiratory and cardiac motion, the variability in myocardial signal related to surface coil intensity inhomogeneity, subendocardial bright signal artifacts caused by stagnant blood, and the subjective nature of T2-STIR image interpretation. We recently introduced direct T2 quantification as an alternative, fast, and accurate method to detect increased T2 values resulting from ischemia-induced myocardial edema that overcomes the aforementioned limitations (9). The current study extends our initial experience with this novel sequence and demonstrates its clinical applicability and robustness in a diverse group of patients presenting with acute coronary syndromes.

The most important finding of our study is that myocardial segments characterized by recent ischemic injury can be quantitatively differentiated from remote myocardium by their higher T2 value. Although the mean difference in T2 between edematous segments and noninfarcted myocardium may appear relatively small in absolute terms (13 ms), a narrow distribution around the mean was found for T2 in remote segments or in myocardium of healthy controls, which resulted in little overlap between ischemic and nonischemic regions. As such, quantitative T2 mapping allowed differentiation of segments with recent ischemic injury in 96% of the patients enrolled in this study. In contrast, T2-STIR clearly was less robust, allowing identification of the infarct region as an area with high signal intensity in only 67% of all patients. Although T2 mapping was similarly effective in showing myocardial edema for STEMI and NSTEMI patients, edema was less frequently detected by T2-STIR in the NSTEMI population. This is important because one can reasonably argue that only NSTEMI patients may eventually benefit from edema-weighted CMR as part of an early risk-stratification strategy.

A significant limitation of T2-STIR imaging in the evaluation of patients with AMI (or myocarditis) is the sensitivity of this sequence to motion, usually related to inadequate breath-holding or an irregular cardiac rhythm. Because of breath-hold problems, T2-STIR images (typically requiring 14 R-R intervals) were uninterpretable in 2 study patients. In contrast, in both of these subjects, it was possible to identify the area of injury by T2 mapping. The relative insensitivity of the T2 mapping technique to motion artifacts is attributable to the nonselective nature of T2 preparation pulse and the fast single-heartbeat SSFP readout, but also by the integrated motion correction algorithm that corrected any image misregistration caused by failed breath-hold or inconsistent cardiac rhythm (Fig. 7).

Our study was not designed to directly compare the predictive accuracy of T2 mapping with T2-STIR imaging; however, our observations do suggest that a T2 value of 62 ms (2 SDs above the mean T2 of normal myocardium) may serve as an appropriate cutoff to differentiate edematous from healthy myocardium.

In a subset of patients, the core of the infarct was found to have a significantly lower T2 value compared with the more peripheral areas of the infarct, which corresponded to the region of MO (no reflow) by LGE imaging. Reperfusion of severely ischemic myocardium may cause intramyocardial hemorrhage by extravasation of red blood cells through the damaged capillaries in the endocardium. The relationship between myocardial hemorrhage and MO was shown in previous studies (18–21), and myocardial hemorrhage is known to

affect T2 relaxation times because of the paramagnetic effects of deoxyhemoglobin contained in the blood degradation products released during reperfusion (22,23). Although we have no direct proof of hemorrhage in our patients with lower T2 at the center of the infarct, the consistency with previous studies demonstrating T2 shortening by hemoglobin breakdown suggests that a similar mechanism is responsible. Other groups have used T2*-weighted gradient-echo techniques to visualize myocardial hemorrhage (18,21), exploiting the sensitivity of this parameter to the paramagnetic effect of iron-containing blood degradation products. It remains to be determined which technique eventually is superior in visualizing myocardial hemorrhage; in acute ischemic injury, quantitative T2 mapping offers the advantage of also depicting tissue edema.

Study limitations

Our sample size was relatively small, although the study population was representative of the spectrum of patients who present with acute coronary syndromes. Despite the small sample size, T2 mapping consistently identified the area of recent myocardial injury with considerably higher values compared with remote and normal myocardium, leading to highly significant results.

The use of a surface coil can be considered as a limitation in our study because the inhomogeneous coil sensitivity profile reduces sensitivity for inferolateral infarction, whereas it may overestimate anteroseptal edema. Attempts have been made to compensate for this problem by using the body-coil receiver, which comes at the cost of a decrease in the signal-to-noise ratio and an increase in scanning time because parallel acquisition techniques cannot be used.

There was some small variability in T2 values found in remote myocardium or in the myocardium of healthy volunteers. Whether these variations between individual patients or between different nonischemic myocardial segments in the same patient are related to small differences in myocardial water content alone or to factors associated with the imaging process itself is currently unknown. Similarly, an even wider distribution of quantitative T2 was observed in the area of myocardial injury. Although it seems reasonable to assume that a higher quantitative T2 can be explained by more pronounced tissue edema, more work is needed to establish the exact mechanisms of this relationship.

Finally, these results were obtained in patients after decision making was essentially complete. Although post-revascularization CMR in STEMI has value in assigning prognosis and may be a useful end point for therapeutic trials of novel cardioprotective agents, the greatest impact on cost-effective care and outcomes may come from incorporating CMR with T2 mapping upfront in the workup of patients presenting with acute chest pain or non-ST elevation acute coronary syndromes. Our group recently showed that qualitative recognition of edema, even with the limitations imposed by STIR imaging before angiography, predicts revascularization need and outcomes (24); this should be even more robust with T2 mapping in these patients. With accruing evidence that an edema-imaging–directed strategy provides incremental information over and beyond other established prognostic markers in patients presenting with possible or established acute coronary

syndrome, T2 mapping may offer a more rapid and reliable approach to edema imaging in the triage and early invasive management of appropriate patients.

CONCLUSIONS

T2 mapping represents a quantitative, robust alternative to conventional T2-STIR imaging to detect myocardial edema in patients presenting with AMI. Incorporation of T2 mapping into CMR protocols may be useful to identify myocardium at risk and MO.

Acknowledgments

The authors thank Saurabh Shah, Dr. Sven Zuehlsdorff, Dr. Xue Hui, and Dr. Jens Guehring of Siemens for their help in implementing the T2-mapping sequence and image-processing algorithm. We also thank Nicholas Dunn for his assistance in analyzing myocardial strain.

Drs. Simonetti and Raman receive research support from Siemens unrelated to this work.

ABBREVIATIONS AND ACRONYMS

AMI	acute myocardial infarction
CI	confidence interval
CMR	cardiac magnetic resonance
LGE	late gadolinium enhancement
LV	left ventricular
MO	microvascular obstruction
NSTEMI	non–ST-segment elevation myocardial infarction
SSFP	steady-state free precession
STEMI	ST-segment elevation myocardial infarction
T2-STIR	T2-weighted short tau inversion recovery

REFERENCES

1. Reimer KA, Jennings RB. The changing anatomic reference base of evolving myocardial infarction. Underestimation of myocardial collateral blood flow and overestimation of experimental anatomic infarct size due to tissue edema, hemorrhage and acute inflammation. Circulation. 1979; 60:866–876. [PubMed: 476891]
2. Abdel-Aty H, Simonetti O, Friedrich M. T2-weighted cardiovascular magnetic resonance imaging. J Magn Reson Imaging. 2007; 26:452–459. [PubMed: 17729358]
3. Friedrich MG. Myocardial edema—a new clinical entity? Nat Rev Cardiol. 2010; 7:292–296. [PubMed: 20309007]
4. Abdel-Aty H, Cocker M, Meek C, Tyberg JV, Friedrich MG. Edema as a very early marker for acute myocardial ischemia: a cardiovascular magnetic resonance study. J Am Coll Cardiol. 2009; 53:1194–1201. [PubMed: 19341860]
5. Aletras AH, Tilak GS, Natanzon A, et al. Retrospective determination of the area at risk for reperfused acute myocardial infarction with T2-weighted cardiac magnetic resonance imaging: histopathological and displacement encoding with stimulated echoes (DENSE) functional validations. Circulation. 2006; 113:1865–1870. [PubMed: 16606793]

6. Friedrich MG, Abdel-Aty H, Taylor A, Schulz-Menger J, Messroghli D, Dietz R. The salvaged area at risk in reperfused acute myocardial infarction as visualized by cardiovascular magnetic resonance. J Am Coll Cardiol. 2008; 51:1581–1587. [PubMed: 18420102]
7. Arai AE. Using magnetic resonance imaging to characterize recent myocardial injury: utility in acute coronary syndrome and other clinical scenarios. Circulation. 2008; 118:795–796. [PubMed: 18711021]
8. Pennell D. Myocardial salvage: retrospection, resolution, and radio waves. Circulation. 2006; 113:1821–1823. [PubMed: 16618830]
9. Giri S, Chung YC, Merchant A, et al. T2 quantification for improved detection of myocardial edema. J Cardiovasc Magn Reson. 2009; 11:56. [PubMed: 20042111]
10. Thygesen K, Alpert JS, White HD, et al. Universal definition of myocardial infarction. Circulation. 2007; 116:2634–2653. [PubMed: 17951284]
11. Simonetti OP, Finn JP, White RD, Laub G, Henry DA. "Black blood" T2-weighted inversion-recovery MR imaging of the heart. Radiology. 1996; 199:49–57. [PubMed: 8633172]
12. Giri S, Xue H, Shah S, et al. Inline non-rigid motion-corrected T2 mapping of myocardium. J Cardiovasc Magn Reson. 2009; 12:P229.
13. Sievers B, Elliott MD, Hurwitz LM, et al. Rapid detection of myocardial infarction by subsecond, free-breathing delayed contrast-enhancement cardiovascular magnetic resonance. Circulation. 2007; 115:236–244. [PubMed: 17200443]
14. Cerqueira MD, Weissman NJ, Dilsizian V, et al. Standardized myocardial segmentation and nomenclature for tomographic imaging of the heart: a statement for healthcare professionals from the Cardiac Imaging Committee of the Council on Clinical Cardiology of the American Heart Association. Circulation. 2002; 105:539–542. [PubMed: 11815441]
15. Hor KN, Gottliebson WM, Carson C, et al. Comparison of magnetic resonance feature tracking for strain calculation with harmonic phase imaging analysis. J Am Coll Cardiol Img. 2010; 3:144–151.
16. Kim RJ, Wu E, Rafael A, et al. The use of contrast-enhanced magnetic resonance imaging to identify reversible myocardial dysfunction. N Engl J Med. 2000; 343:1445–1453. [PubMed: 11078769]
17. Cury RC, Shash K, Nagurney JT, et al. Cardiac magnetic resonance with T2-weighted imaging improves detection of patients with acute coronary syndrome in the emergency department. Circulation. 2008; 118:837–844. [PubMed: 18678772]
18. Asanuma T, Tanabe K, Ochiai K, et al. Relationship between progressive microvascular damage and intramyocardial hemorrhage in patients with reperfused anterior myocardial infarction: myocardial contrast echocardiographic study. Circulation. 1997; 96:448–453. [PubMed: 9244211]
19. Beek AM, Nijveldt R, van Rossum AC. Intramyocardial hemorrhage and microvascular obstruction after primary percutaneous coronary intervention. Int J Cardiovasc Imaging. 2010; 26:49–55. [PubMed: 19757151]
20. Kloner RA, Ganote CE, Jennings RB, Reimer KA. Demonstration of the "no-reflow" phenomenon in the dog heart after temporary ischemia. Recent Adv Stud Cardiac Struct Metab. 1975; 10:463–474. [PubMed: 1208994]
21. Ochiai K, Shimada T, Murakami Y, et al. Hemorrhagic myocardial infarction after coronary reperfusion detected in vivo by magnetic resonance imaging in humans: prevalence and clinical implications. J Cardiovasc Magn Reson. 1999; 1:247–256. [PubMed: 11550358]
22. Lotan CS, Bouchard A, Cranney GB, Bishop SP, Pohost GM. Assessment of postreperfusion myocardial hemorrhage using proton NMR imaging at 1.5 T. Circulation. 1992; 86:1018–1025. [PubMed: 1516171]
23. Lotan CS, Miller SK, Cranney GB, Pohost GM, Elgavish GA. The effect of postinfarction intramyocardial hemorrhage on transverse relaxation time. Magn Reson Med. 1992; 23:346–355. [PubMed: 1549048]
24. Raman SV, Simonetti OP, Winner MW, et al. Cardiac magnetic resonance with edema imaging identifies myocardium at risk and predicts worse outcome in patients with non–ST-segment elevation acute coronary syndrome. J Am Coll Cardiol. 2010; 55:2480–2488. [PubMed: 20510215]

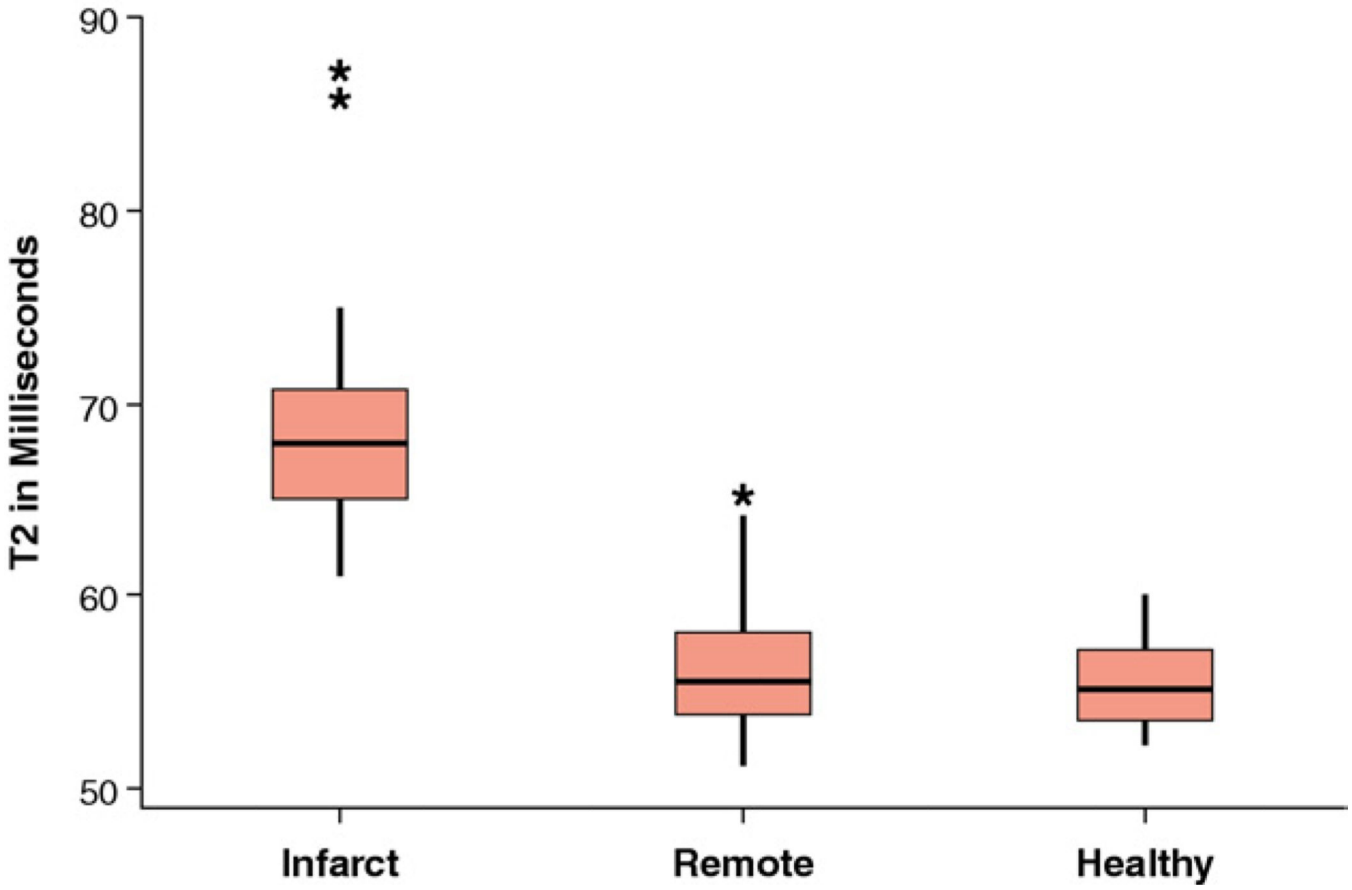

Figure 1. Quantitative T2 in Infarct Zone, Remote and Healthy Control Myocardium

Box plot displays the distribution of quantitative T2 values measured within the infarct zone, remote myocardium, and myocardium of healthy controls. Whisker lengths define the distance between the 25th and the 75th percentiles.

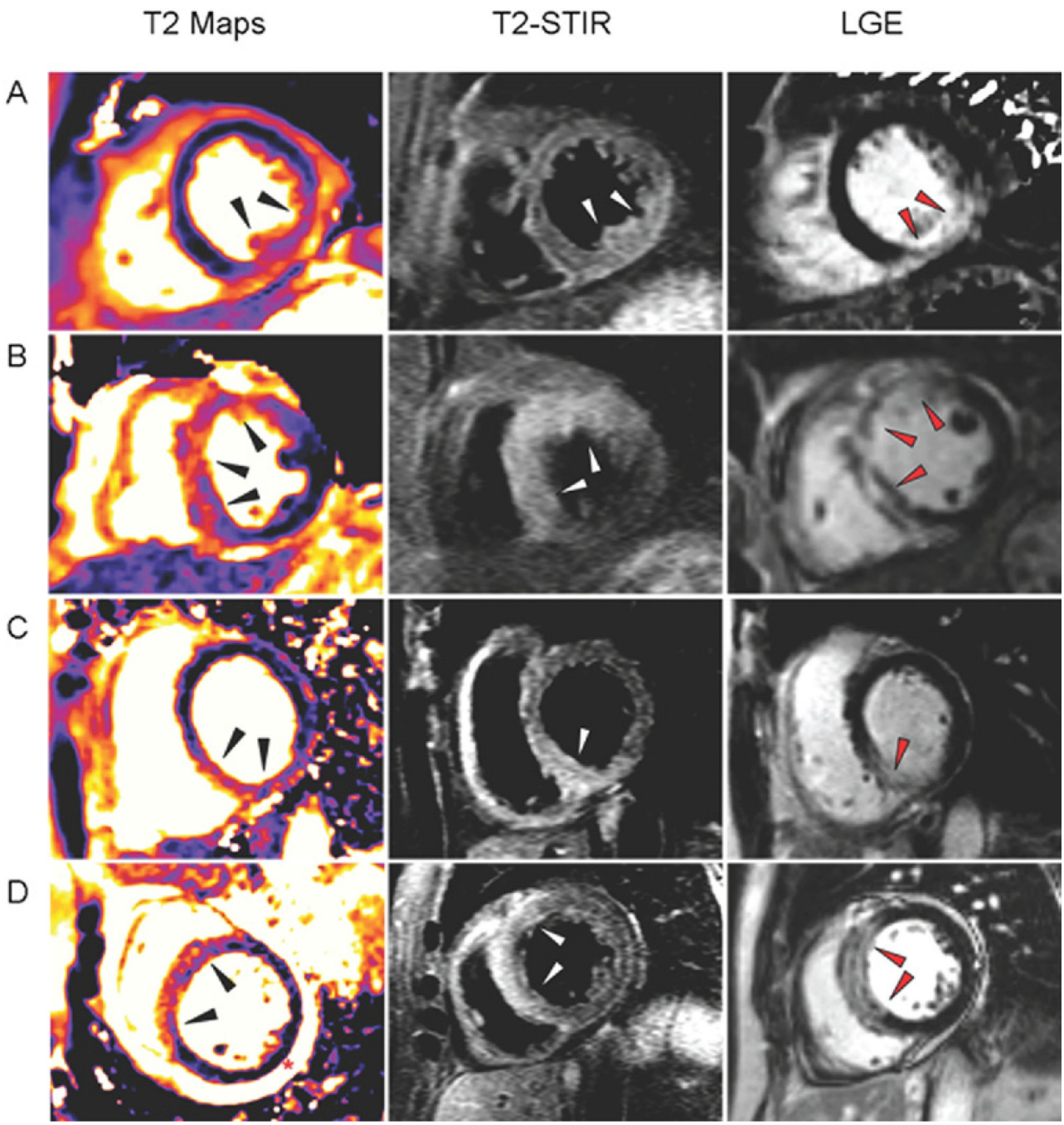

Figure 2. T2 Maps, T2-STIR, and LGE Images in Patients With AMI

(A) A 53-year-old male patient admitted with ST-segment elevation myocardial infarction (STEMI) in the circumflex artery territory. Quantitative T2 in the infarct region was 72 ms compared with 56 ms in remote myocardium. **(B)** A 75-year-old-male patient presenting with left anterior descending artery territory STEMI. T2 of the infarct zone measured by T2 mapping was 66 ms compared with 51 ms in remote myocardium. **(C)** Basal short-axis slice in a 58-year-old female patient presenting with non-STEMI in the right coronary artery territory. T2 measured within the region of the infarct was 71 ms compared with 58 ms in

remote myocardium. **(D)** A 62-year-old male patient admitted with a STEMI in the left anterior descending artery territory. Quantitative T2 of the infarcted segments was 73 ms. By T2 mapping, a rim with high signal intensity circumferential to the left ventricle is seen (*****), consistent with post-infarct pericardial effusion. The region of infarct is indicated by **arrowheads**. AMI = acute myocardial infarction; LGE = late gadolinium enhancement; T2-STIR = T2-weighted short tau inversion recovery.

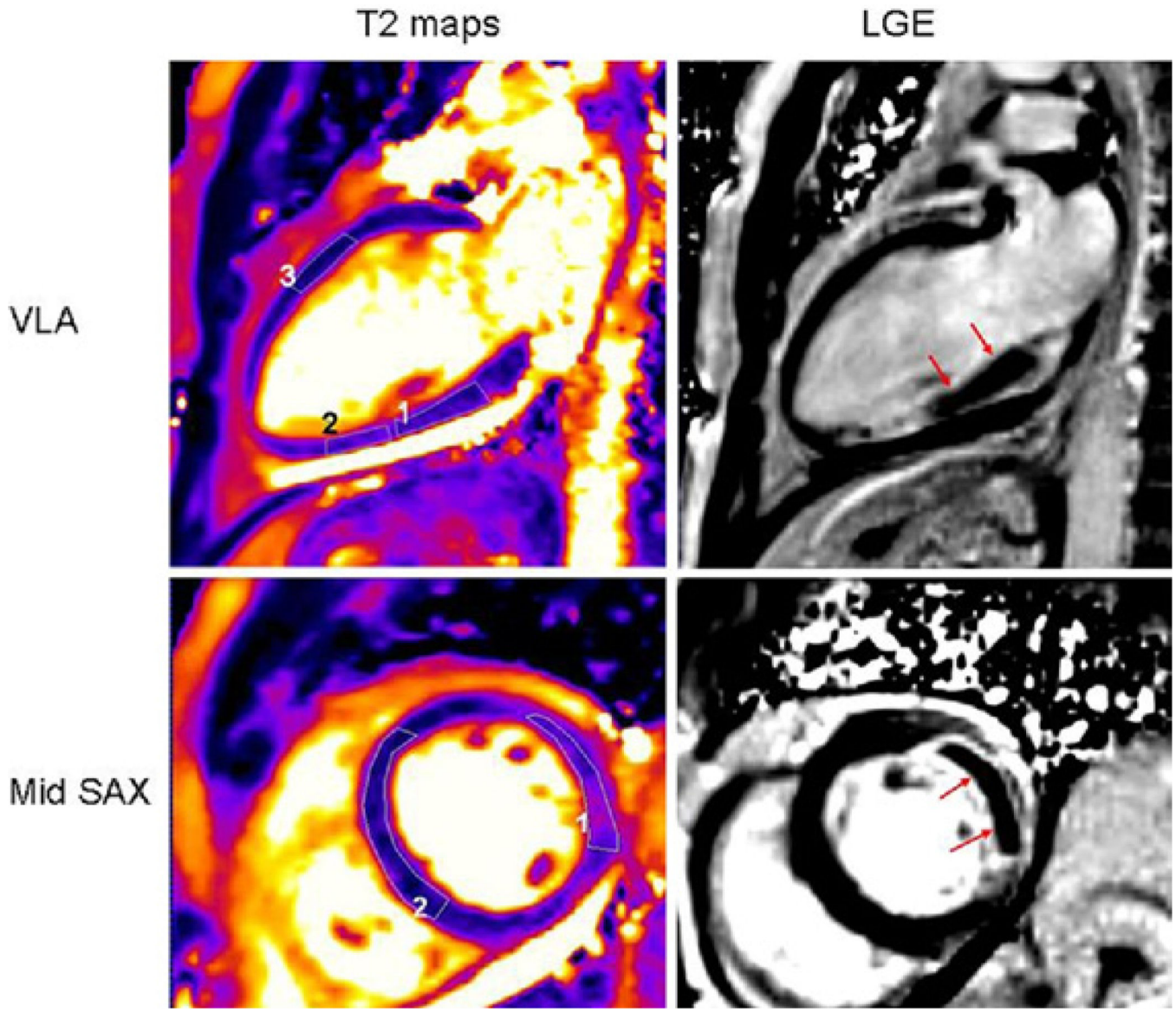

Figure 3. T2 Maps and LGE Images in Circumflex Artery Territory STEMI

Cardiac magnetic resonance was performed in this 51-year-old patient shortly after percutaneous revascularization. With LGE imaging, a large area of microvascular obstruction **(red arrows)** was observed, which corresponded to relatively low T2 values measured by quantitative T2 analysis. Vertical long-axis (VLA) view: T2 region 1, 57 ms; T2 region 2, 65 ms; T2 region 3, 54 ms. Mid-ventricular short-axis (Mid SAX) view: T2 region 1, 59 ms; T2 region 2, 54 ms. Abbreviations as in Figure 2.

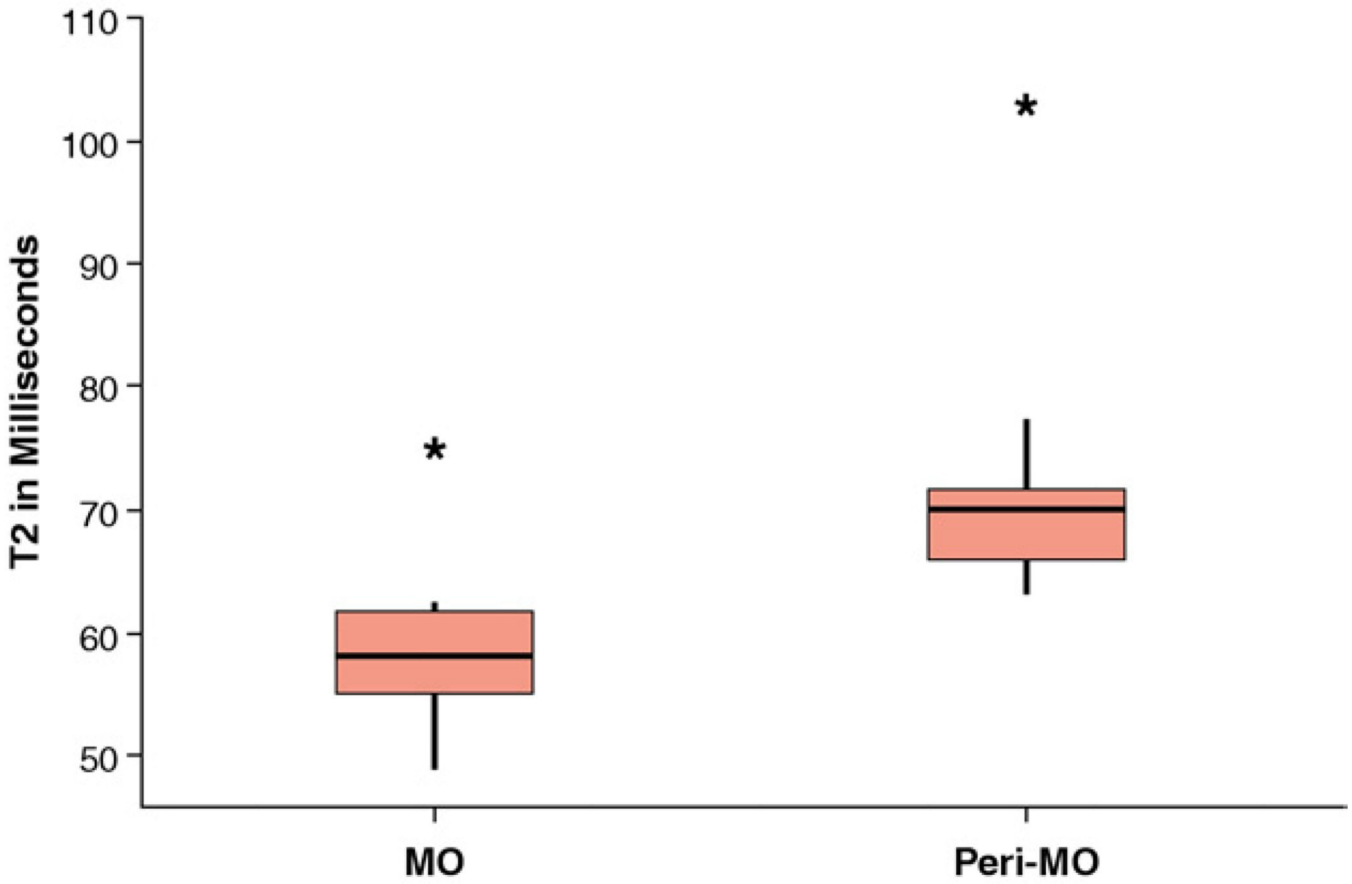

Figure 4. Quantitative T2 in MO and Infarct Tissue Beyond MO

Box plot comparing T2 values observed in areas of microvascular obstruction (MO) and infarct tissue outside the area of MO. Whisker lengths define the distance between the 25th and the 75th percentile. **Asterisks** indicate outliers.

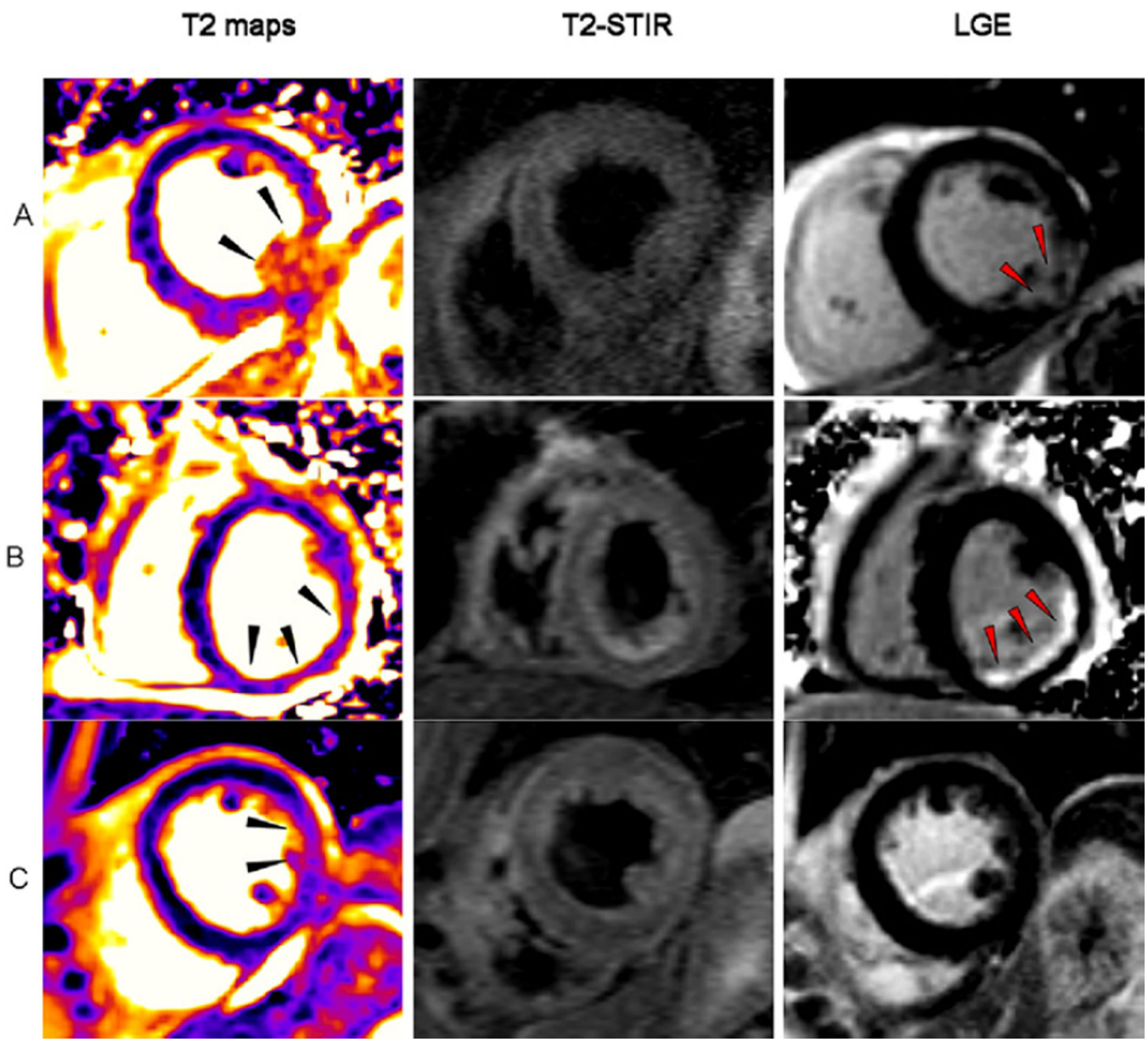

Figure 5. Matching T2 Maps, T2-STIR, and LGE Images in Patients With AMI and No Obvious Edema by T2-STIR

The region of infarct is indicated by **arrowheads. (A)** A 62-year-old male patient with non–ST-segment myocardial infarction (NSTEMI) (chest pain and minimally increased troponin I levels on admission). Findings on the coronary angiogram were initially interpreted as negative, but on further review (because of LGE images indicating a small region of infarct scar, [**red arrowheads**]), a lesion was found at the ostium of the third marginal branch of the right coronary artery. Findings on T2-STIR images were negative, but the T2 maps demonstrated focal tissue edema in the mid-inferolateral segment (T2 = 67 ms), involving the posteromedial papillary muscle. **(B)** A 60-year-old male patient presenting with NSTEMI; LGE images demonstrated a subendocardial infarct in the circumflex artery territory, corresponding to a focal “hotspot” by T2 mapping (T2 within the infarct = 68 ms).

T2-STIR images could not definitively demarcate the area of injury due to subendocardial bright signal caused by stagnant blood. **(C)** A 45-year-old female patient with STEMI, undergoing percutaneous coronary intervention of the mid-circumflex artery territory shortly after onset of symptoms. Early successful revascularization resulted in the absence of irreversible myocardial injury by LGE 2 days later. T2-STIR images showed no enhancement; T2 maps, however, unequivocally indicated edema in the mid-inferolateral segment (T2 = 69 ms). Abbreviations as in Figure 2.

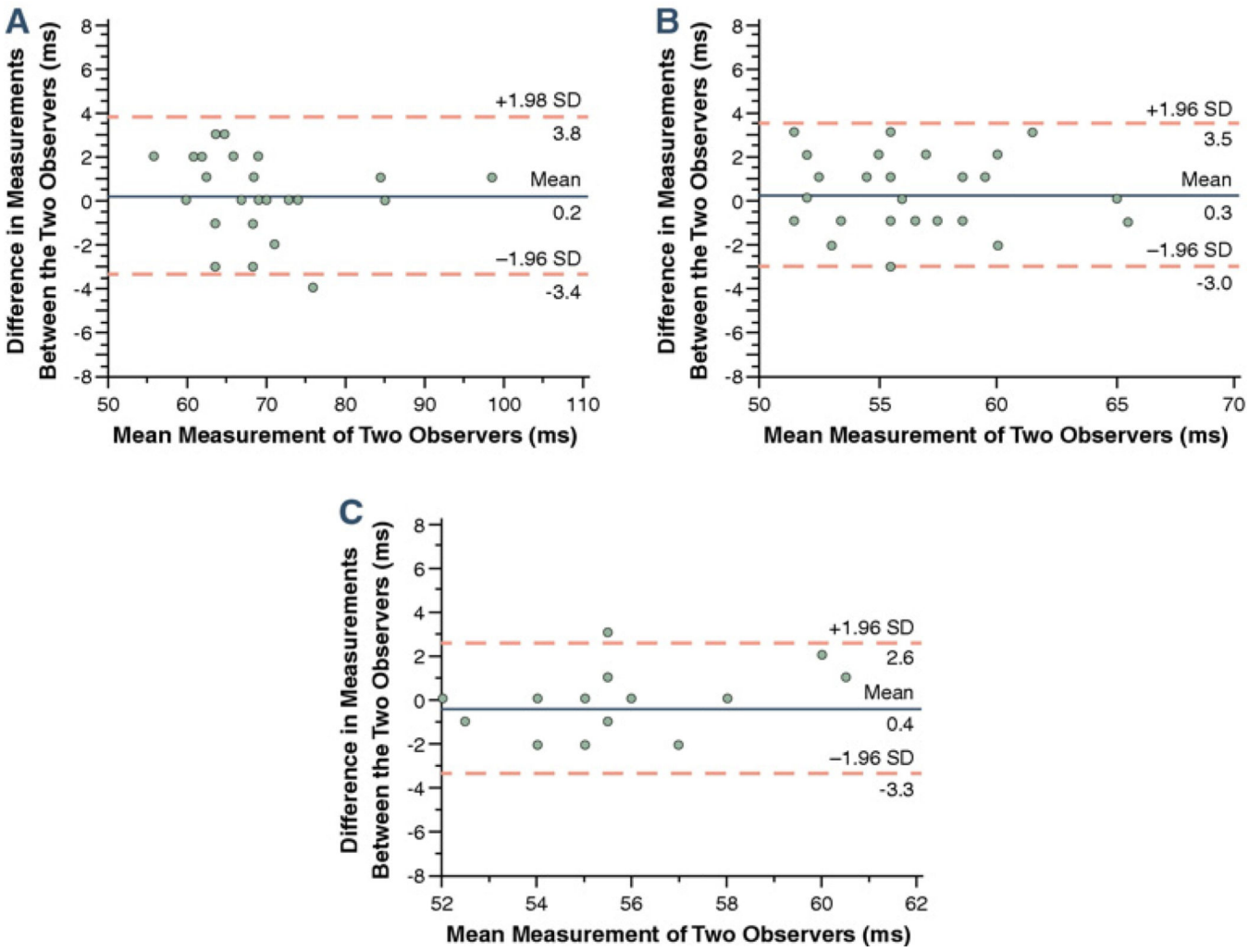

Figure 6. Bland-Altman Plots of Interobserver T2 Measurement Agreement

Bland-Altman plots for the measurement of quantitative T2 in infarcted myocardium **(A)**, remote myocardium **(B)**, and healthy controls **(C)**, showing good interobserver agreement. Sample size in **(C)** = 21, with overlapping data causing dots standing for >1 data point.

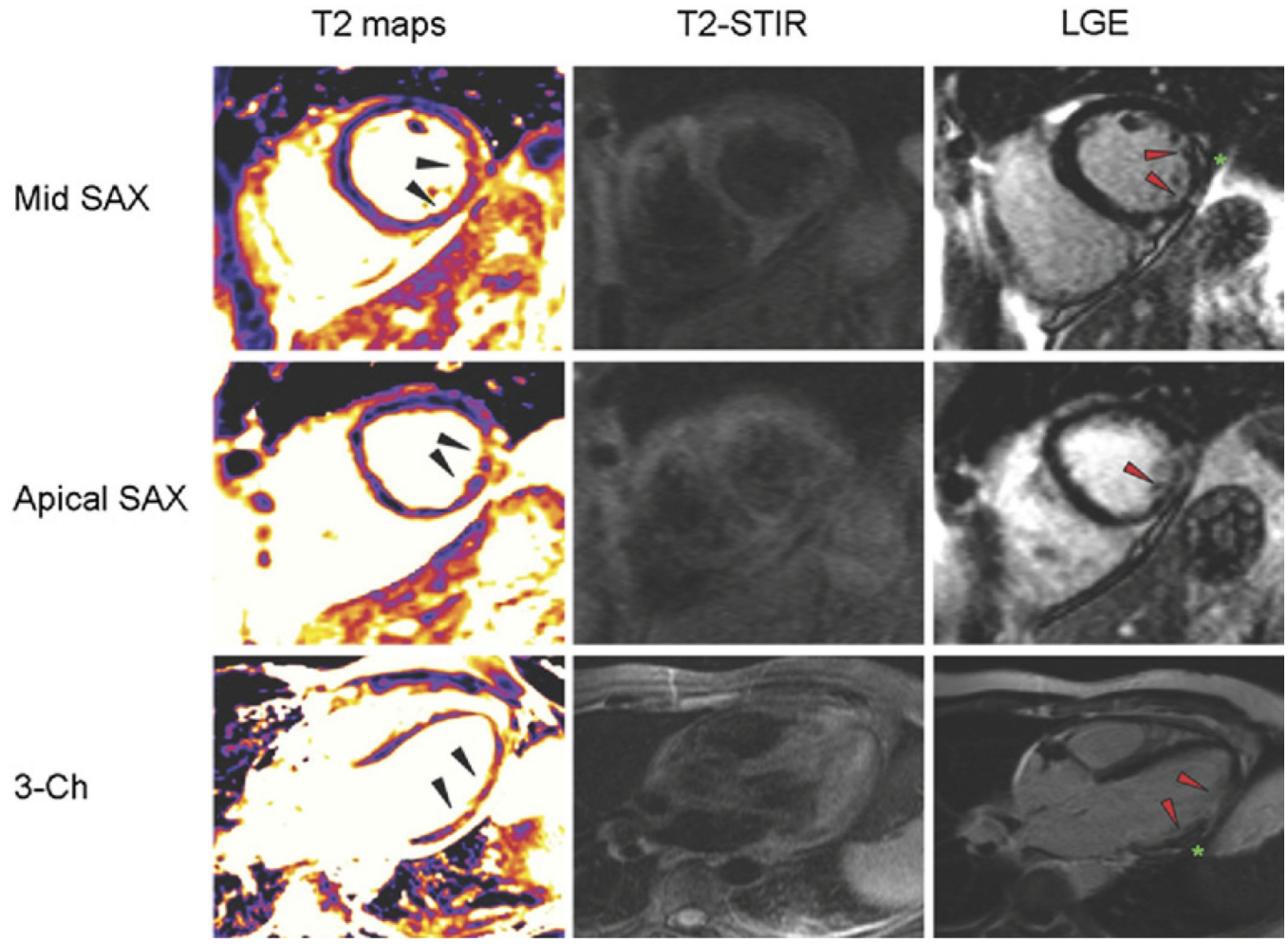

Figure 7. T2 Maps, T2-STIR, and Single Heartbeat LGE Images Acquired With Free Breathing

This 48-year-old patient with AMI due to thrombotic occlusion of the right coronary artery was allowed to breath freely during the cardiac magnetic resonance examination. T2-STIR images were heavily degraded by motion artifacts, but T2 maps remained diagnostic, showing injury in the inferolateral segments **(arrowheads)**. Quantitative T2 measured in the infarct zone outside the MO area **(*)** was 67 ms. Mid/apical SAX = mid ventricular/apical short-axis view; 3-Ch = 3-chamber view; other abbreviations as in Figure 2.

Table 1

Cardiovascular Magnetic Resonance Parameters

Sequence	**B-SSFP CINE**		**T2-STIR**	**T2 Maps**	**LGE**	
Breatd-hold	Yes (segmented)	No (real-time cines)*	Yes	Yes	Yes (segmented)	No (single shot)*
Parallel acceleration	GRAPPA rate 2	TSENSE rate 3	GRAPPA rate 2	GRAPPA rate 2	None	GRAPPA rate 2
In-plane resolution, mm	1.5 × 1.5	3.5 × 2.1	2.2 × 1.5	2.2 × 2.8	2.2 × 2.0	2.5 × 1.9
Slice thickness, mm	8	8	8	8	8	8
TR/TE, ms	3.0/1.3	2.3/1.0	2 × R-R/60	3 × R-R/0, 24, 60	1 × R-R/4.2	2.8 /1.1
Bandwidth, Hz/pixel	930	1,630	930	1,445	130	1,150
Flip angle, °	65	74	180	40	25	40

*In subjects with limited breath-hold capacity.

B-SSFP = balanced steady-state free precession imaging; GRAPPA = generalized autocalibrating partially parallel acquisition; LGE = late gadolinium enhancement; T2-STIR = T2-weighted short tau inversion recovery; TE = echo time; TR = repetition time; TSENSE = time-adaptive sensitivity encoding.

Table 2

Baseline Characteristics of the Study Population (N = 27)

Variable	Value
Age, yrs	61 ± 12
Male/female, n	16/11
White, n (%)	23 (85)
Hypertension, n (%)	19 (70)
Hyperlipidemia, n (%)	17 (63)
Smoking history: current/former/never, n (%)	5/8/14 (18/30/52)
Diabetes, n (%)	8 (30)
Body mass index, kg/m^2	30.0 ± 5.8
Previous myocardial infarction, n (%)	2 (7)
Previous CABG, n (%)	2 (7)
Previous PCI	0
STEMI/NSTEMI, n (%)	16/11 (59/41)
Peak troponin I, mg/dl, median (IQR)	50 (13.8–96.0)
Culprit coronary artery, n	
Left anterior descending	6
Right coronary artery	11
Circumflex artery	10
Days ± SD between admission and CMR	2.1 ± 1.3
Revascularization, n (%)	
CABG	1 (4)
PCI	19 (70)
None	7 (26)

CABG = coronary artery bypass grafting; CMR = cardiac magnetic resonance; IQR = interquartile range; PCI = percutaneous coronary intervention; NSTEMI = non–ST-segment elevation myocardial infarction; STEMI = ST-segment elevation myocardial infarction.

Table 3

General CMR Findings

Variable	Value
LV end-diastolic volume index, ml/m^2	77 ± 20
LV end-systolic volume index, ml/m^2	41 ± 20
LV ejection fraction, %	49 ± 12
LV mass index, mg/m^2	71 ± 18
Wall motion score index, median (IQR)	0.75 (0.43–1.19)
LGE score, median (IQR)	12 (4–24)
Peak circumferential strain, remote myocardium, %	−24.6 ± 7.8
Peak circumferential strain, infarct zone, %	−13.7 ± 5.5*
Peak radial strain, infarct zone, %	43.2 ± 11.5
Peak radial strain, remote myocardium, %	18.8 ± 8.0*

* $p < 0.0001$ for difference with infarct zone.

LGE = late gadolinium enhancement; LV = left ventricular; other abbreviations as in Table 2.